

SINGLE-STEP TRAVELING-WAVE QUANTUM STATE ENGINEERING IN THE COHERENT STATE REPRESENTATION

Gabor Mogyorosi,¹ Emese Molnar,¹ Matyas Mechler,¹ and Peter Adam^{1,2*}

¹*Institute of Physics, University of Pécs
Ifjúságútja 6, Pécs H-7624, Hungary*

²*Institute for Solid State Physics and Optics
Wigner Research Centre for Physics, Hungarian Academy of Sciences
Budapest H-1525, P.O. Box 49, Hungary*

*Corresponding author e-mail: adam.peter@wigner.mta.hu

Abstract

We describe a recently introduced single-step traveling-wave quantum state engineering scheme using the one-dimensional coherent-state representation introduced by Janszky. In this representation, the photon number expansion of the output state is derived in a compact formula that is advantageous for numerical optimization. Using this formula, we determine several sets of physically controllable parameters of the scheme yielding various nonclassical target states.

Keywords: one-dimensional coherent state representation, quantum state engineering, nonclassical states.

1. Introduction

There exists a persistent interest on the generation of nonclassical states of light due to their essential role in numerous applications in quantum optics and quantum information processing. The preparation of nonclassical states in traveling optical modes is generally required for many practical applications. An efficient method for this task is measurement-induced conditional preparation, where one of the modes of a bipartite correlated state is measured, thereby projecting the state of the other mode to the desired one. The majority of the conditional schemes is developed for the generation of a certain state. For example, optical cat states and their squeezed versions have been successfully generated experimentally in such protocols [1–6].

The aim of quantum state engineering is the generation of a variety of nonclassical states in the same experimental scheme. A plausible approach for the engineering is the systematic construction of the photon number expansion of the quantum states up to a given photon number. The methods developed for this task are based on repeated photon additions [7], photon subtractions [8], and various combinations of these [9, 10]. Another kind of engineering is based on the discrete coherent state superpositions approximating the target states [11]. Such superpositions have been introduced and analyzed by Janszky et al. [12–15].

The problem of the former approach is that the number of detection events and optical elements is generally proportional to the amount of number states involved in the photon number expansion of the

target state leading to a decrease in the success probability and even to that fidelity of the preparation of states involving larger photon number components. The arrangements applying the latter approach contain only a few elements and measurements, which partly overcomes this issue. However, they still exhibit only a moderate success probability, owing to the application of multiple measurements.

Recently, a single-step quantum state engineering scheme has been proposed for the high-fidelity conditional generation of a large variety of nonclassical states of traveling optical fields [16]. It contains only a single measurement leading to high success probabilities. In this scheme, the physically controllable parameters of the arrangement encode the generated state, and they can be determined by numerical optimization.

In this paper, we develop the description of this single-step scheme using the one-dimensional coherent-state representation introduced by Janszky [17]. One-dimensional coherent state representations are defined on certain contours such as straight lines and circles in the phase space that is on the α plane [17–23]. Such representations have been determined for several relevant nonclassical states including squeezed coherent states [17, 18], amplitude squeezed states [19, 21], and squeezed displaced number states [22]. A systematic method to obtain the straight-line coherent-state distribution function for a given state has also been developed [20]. This representation is not unique due to the overcompleteness of the coherent states [20, 23]. Due to its relative simplicity, it proved to be a useful mathematical tool for describing nonclassical states and treating optical processes [24].

In the end, using the developed description for numerical optimization, we show that various classes of nonclassical states can be generated with high fidelity and success probability in the considered scheme. Our novel examples include amplitude squeezed states, special photon number superpositions, and optical cat states.

This paper is organized as follows.

In Sec. 2, we present the considered single-step quantum state engineering method and derive the output state by applying one-dimensional coherent state representations for the input states. In Sec. 3, we present and discuss the results of the numerical optimization for a wide variety of target states. Finally, we conclude in Sec. 4.

2. Description of the Scheme in One-Dimensional Representation

In [16], a single-step conditional quantum state engineering scheme was presented with two alternative measurements. In this paper, we analyze the version of that scheme containing a single photon detector (SPD) using one-dimensional coherent state representations.

The considered scheme is presented in Fig. 1. Two squeezed coherent states $|\zeta_j, \alpha_j\rangle$ with squeezing factors $\zeta_j = r_j \exp(i\theta_j)$ and coherent amplitudes $\alpha_j = |\alpha_j| \exp(i\phi_j)$ ($j = 1, 2$) overlap with a beam splitter of transmittance T . After the beam splitter a single photon detection (SPD) is performed on one of the outputs to herald the generation of the desired output state $|\psi_{\text{out}}\rangle$ on the other mode.

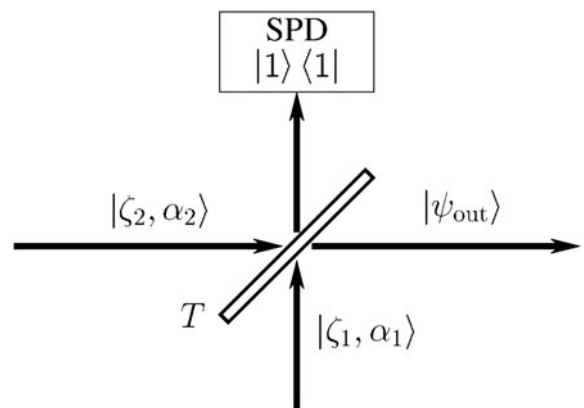


Fig. 1. Experimental scheme for generating a wide variety of nonclassical states in traveling optical field. The input squeezed coherent states $|\zeta_i, \alpha_i\rangle$ interfere on a beam splitter with transmittance T .

Squeezed coherent states $|\zeta, \alpha\rangle$ can be derived from the vacuum state by the consecutive application of the squeezing operator $\hat{S}(\zeta)$ and the displacement operator $\hat{D}(\alpha)$ as $|\zeta, \alpha\rangle = \hat{D}(\alpha)\hat{S}(\zeta)|0\rangle$. These states can be described by various straight-line superpositions. The simplest one is defined along a straight line in the phase space crossing the coherent state appearing in the definition, and the direction of the line is perpendicular to the direction of the squeezing. In this case, the one-dimensional representation of the state reads as [18]

$$|\zeta, \alpha\rangle = \frac{1}{\sqrt{\pi}} \int g(x)|\alpha + \gamma x\rangle dx, \tag{1}$$

where

$$g(x) = \frac{1}{\sqrt{2 \sinh(r)}} \exp \left[-\frac{1}{2}(\coth(r) - 1)x^2 + \left(\frac{\alpha\gamma^* - \alpha^*\gamma}{2} \right) x \right], \quad \gamma = \exp \left(\frac{i\theta}{2} \right). \tag{2}$$

This means that the squeezed coherent state is the Gaussian superposition of the coherent states along the given line.

The advantage of the coherent state representation is that for coherent inputs the beam splitter transformation for a beam splitter with transmittance T can be given in the following simple form:

$$|\alpha\rangle_1 \otimes |\beta\rangle_2 \rightarrow \left| \sqrt{T}\alpha + \sqrt{1-T}\beta \right\rangle_3 \otimes \left| \sqrt{1-T}\alpha - \sqrt{T}\beta \right\rangle_4. \tag{3}$$

Using the representation (1) of the input states and applying the formula $\langle 1|\alpha\rangle = \alpha \exp(-|\alpha|^2/2)$, the output state of the system after the measurement can be written as

$$|\psi_{\text{out}}\rangle_{\text{SPD}} = \mathcal{N}C_{\text{SPD}}(\alpha_1, \alpha_2, T) \iint g_{\text{SPD}}(x, y) \left| \sqrt{1-T}(\alpha_1 + \gamma_1 x) - \sqrt{T}(\alpha_2 + \gamma_2 y) \right\rangle dx dy, \tag{4}$$

where

$$\begin{aligned} g_{\text{SPD}}(x, y) = & \left[\sqrt{1-T}(\alpha_1 + \gamma_1 x) + \sqrt{T}(\alpha_2 + \gamma_2 y) \right] \\ & \times \exp \left\{ -\frac{1}{2} \left[(\coth(r_1) - 1 + T)x^2 + (\coth(r_2) - T)y^2 \right. \right. \\ & + \left(T(\alpha_1^* \gamma_1 + \alpha_1 \gamma_1^*) + \sqrt{T(1-T)}(\alpha_2^* \gamma_1 + \alpha_2 \gamma_1^*) \right) x \\ & + \left([1-T](\alpha_2^* \gamma_2 + \alpha_2 \gamma_2^*) + \sqrt{T(1-T)}(\alpha_1^* \gamma_2 + \alpha_1 \gamma_2^*) \right) y \\ & \left. \left. + \sqrt{T(1-T)}(\gamma_1^* \gamma_2 + \gamma_1 \gamma_2^*) xy \right] \right\} \end{aligned} \tag{5}$$

and

$$\begin{aligned} C_{\text{SPD}}(\alpha_1, \alpha_2, T) = & \frac{1}{2\pi \sqrt{\sinh(r_1) \sinh(r_2)}} \\ & \times \exp \left\{ -\frac{1}{2} \left[T|\alpha_1|^2 + (1-T)|\alpha_2|^2 + \sqrt{T(1-T)}(\alpha_1^* \alpha_2 + \alpha_1 \alpha_2^*) \right] \right\}. \end{aligned} \tag{6}$$

According to Eq. (4), the output state $|\psi_{\text{out}}\rangle_{\text{SPD}}$ is described by a special two-dimensional coherent state representation defined on the phase space.

Applying Eqs. (4)–(6) and the formula $\langle n | \alpha \rangle = (\alpha^n / \sqrt{n!}) \exp[-|\alpha|^2/2]$, the photon number expansion

$$|\psi_{\text{out}}\rangle_{\text{SPD}} = \mathcal{N} \sum_{n=0}^{\infty} c_n^{(\text{SPD})} |n\rangle \tag{7}$$

can be easily derived. The coefficients read

$$\begin{aligned} c_n^{(\text{SPD})} = C'_{\text{SPD}}(\alpha_1, \alpha_2, T) & \iint [\sqrt{1-T}(\alpha_1 + \gamma_1 x) + \sqrt{T}(\alpha_2 + \gamma_2 y)] \\ & \times [\sqrt{1-T}(\alpha_1 + \gamma_1 x) - \sqrt{T}(\alpha_2 + \gamma_2 y)]^n \\ & \times \exp \left\{ -\frac{1}{2} \left[(\coth(r_1) - 1 + T) x^2 + (\coth(r_2) - T) y^2 \right. \right. \\ & \left. \left. + 2T (\alpha_1^* \gamma_1 + \alpha_1 \gamma_1^*) x + 2[1-T] (\alpha_2^* \gamma_2 + \alpha_2 \gamma_2^*) y \right] \right\} dx dy, \end{aligned} \tag{8}$$

where

$$C'_{\text{SPD}}(\alpha_1, \alpha_2, T) = \frac{1}{2\pi \sqrt{\sinh(r_1) \sinh(r_2)} n!} \exp \left\{ -[T|\alpha_1|^2 + (1-T)|\alpha_2|^2] \right\}. \tag{9}$$

Even though these coefficients are defined through a two-dimensional integral, the derived formula is much simpler than the one defined in [16] and can be efficiently used for numerical optimization.

3. Generation of Nonclassical States

In this section, we demonstrate through examples how the scheme can be applied to generate a large variety of nonclassical states. Our examples include amplitude squeezed states, resource states, special photon number state superpositions, and optical cat states. The latter states are not considered in [16].

Amplitude squeezed states are defined by Gaussian continuous coherent state superpositions on circles in the phase space,

$$|\alpha_0, u, \delta\rangle_A = \mathcal{N} \int \exp \left(-\frac{1}{2} u^2 \phi^2 - i\delta\phi \right) |\alpha_0 e^{i\phi}\rangle d\phi, \tag{10}$$

where \mathcal{N} is a normalization constant, u determines the width of the distribution, α_0 is the magnitude of the amplitudes of the superposed coherent states, and δ is a free modulation constant. Amplitude squeezed states contract into the coherent state $|\alpha_0\rangle$ in the limit $u \rightarrow \infty$, while in the opposite limit $u \ll 1$, an n -photon number state with $n = \delta$ is achieved. The state $|\alpha_0, u, \delta\rangle_A$ can be expanded in the photon number basis as

$$|\alpha_0, u, \delta\rangle_A = \mathcal{N} \sum_{n=0}^{\infty} \frac{\sqrt{2\pi} \alpha_0^n}{u \sqrt{n!}} \exp \left[-\frac{(\delta - n)^2}{2u^2} \right] |n\rangle. \tag{11}$$

These states are intelligent states of the Pegg–Barnett–number–phase uncertainty relation and also of an alternative to this relation introduced as the number-operator–annihilation operator uncertainty relation for a certain parameter range [19,25,26]. Hence, they can be used for testing various uncertainty relations experimentally.

We also consider the following superpositions of photon number states with *ad hoc* coefficients,

$$\begin{aligned}
 |\psi_{01}\rangle &= \frac{1}{\sqrt{2}}(|0\rangle + |1\rangle), & |\psi_{12}\rangle &= \frac{1}{\sqrt{5}}(2|1\rangle + |2\rangle), \\
 |\psi_{135}\rangle &= \mathcal{N}(|1\rangle + 0.2|3\rangle + 0.1|5\rangle), & |\psi_{012}\rangle &= \mathcal{N}(2|0\rangle + |1\rangle + 0.5|2\rangle),
 \end{aligned}
 \tag{12}$$

and the special superposition

$$|\psi(\zeta, \chi')\rangle_{\text{R}} = \hat{S}(\zeta) \left(|0\rangle + \chi' \frac{3}{2\sqrt{2}}|1\rangle + \chi' \frac{\sqrt{3}}{2}|3\rangle \right)
 \tag{13}$$

referred to as resource states that can be used for realizing cubic nonlinear quantum gates essential for universal continuous-variable quantum computation in the optical setting [27–29].

We will also consider optical even cat states defined as $|\alpha\rangle_{\text{C}} = \mathcal{N}(|\alpha\rangle + |-\alpha\rangle)$. These states and their odd versions form a basis for linear optical quantum computing [30, 31].

The photon number expansion presented in Eqs. (8) and (9) contains nine adjustable parameters; these are: the complex squeezing parameters ζ_j and the complex coherent signals α_j of the input squeezed coherent states, and the transmittance T of the beam splitter. In order to generate a given target state, our task is to find the values of the variable parameters of the introduced scheme for which the misfit $\varepsilon = 1 - |\langle \psi_{\text{out}} | \psi_{\text{target}} \rangle|^2$ between the target state $|\psi_{\text{target}}\rangle$ and the generated states $|\psi_{\text{out}}\rangle$ is minimal. We used a genetic algorithm [32] to solve this optimization problem. We imposed bounds on the variables so that their values are physically reasonable while the optimization problem is numerically stable and

Table 1. Results of the Optimization for Different Nonclassical States for the Scheme of Fig. 1.^a

state	ε	r_1	θ_1	α_1	ϕ_1	r_2	θ_2	α_2	ϕ_2	T	P
$ 1, 0.8, 1\rangle_{\text{A}}$	$1.15 \cdot 10^{-4}$	0.36	0.40	0.50	4.89	0.54	0.34	0.12	4.93	0.45	0.202
$ \sqrt{2}, 2, 2\rangle_{\text{A}}$	$4.07 \cdot 10^{-3}$	0.61	3.16	1.49	4.94	0.34	2.14	0.63	5.08	0.27	0.364
$ \sqrt{2}, 5, 2\rangle_{\text{A}}$	$2.05 \cdot 10^{-4}$	0.33	2.68	1.39	4.29	0.96	2.68	1.04	1.72	0.18	0.269
$ 2, 5, 4\rangle_{\text{A}}$	$1.29 \cdot 10^{-4}$	0.06	2.31	2.01	4.52	0.24	0.10	0.90	0.46	0.49	0.386
$ \Psi(0.15, 0.05)\rangle_{\text{R}}$	$3.80 \cdot 10^{-4}$	0.25	5.53	0.50	3.92	0.27	5.68	0.55	2.53	0.55	0.293
$ \Psi(0.1, 0.1)\rangle_{\text{R}}$	$1.83 \cdot 10^{-3}$	0.34	5.20	0.50	3.25	0.90	4.90	1.5	1.23	0.29	0.217
$ \Psi(-0.25, 0.1)\rangle_{\text{R}}$	$1.83 \cdot 10^{-3}$	0.49	2.01	0.80	1.08	0.77	2.87	0.98	5.95	0.71	0.284
$ \Psi(0.1i, 0.15)\rangle_{\text{R}}$	$4.32 \cdot 10^{-3}$	0.36	1.64	0.58	0.60	0.55	2.30	0.45	5.23	0.62	0.314
$ \Psi(0.4, 0.2)\rangle_{\text{R}}$	$7.75 \cdot 10^{-3}$	0.74	1.55	1.37	5.71	0.51	0.94	0.69	4.59	0.63	0.196
$ \psi_{01}\rangle$	$7.91 \cdot 10^{-6}$	0.25	4.90	0.20	3.57	0.27	4.92	0.19	1.50	0.48	0.111
$ \psi_{12}\rangle$	$2.63 \cdot 10^{-3}$	0.63	4.26	0.34	4.13	0.95	4.53	0.64	0.57	0.41	0.226
$ \psi_{135}\rangle$	$3.41 \cdot 10^{-3}$	0.32	5.94	0	0.73	0.44	5.21	0	1.57	0.22	0.072
$ \psi_{012}\rangle$	$2.09 \cdot 10^{-3}$	0.38	6.25	0.91	5.59	0.67	0.50	1.29	4.90	0.44	0.233

^aThe table presents for each state the minimal misfit ε and the corresponding optimal choice of parameters: the parameters of the input squeezed coherent states ($r_1, \theta_1, \alpha_1, \phi_1, r_2, \theta_2, \alpha_2$, and ϕ_2), the transmittance of the beam splitter T , and the success probability P .

feasible. The applied ranges are $0 < r_i \leq 1.5$, $0 \leq \alpha_i \leq 2$, $0.1 \leq T \leq 0.9$, and all the phase angles θ_i and ϕ_i are allowed to take any possible values between 0 and 2π . We also calculated the probability of success of the generation for each of the analyzed states. This quantity is another figure of merit characterizing the performance of a conditional scheme. In the case of SPD, it is defined as $P = \text{Tr}(\hat{\rho}_3|1\rangle\langle 1|)$, where $\hat{\rho}_3 = \text{Tr}_4(|\psi_{\text{out}}\rangle_{34}\langle\psi_{\text{out}}|)$ is the density operator of the mode on which the measurement is performed. The two-mode output state after the beam splitter is the state $|\psi_{\text{out}}\rangle_{34}$ not presented here explicitly.

In Table 1, we present the results of the optimization for several examples for the amplitude squeezed states and for the special photon number superpositions defined in Eqs. (12) and (13) prepared in the scheme. The examples show that all these states can be generated with high fidelities, that is, low misfits by the proposed conditional scheme. The achievable success probabilities of the generation are rather high compared to the ones that can be typically achieved in other quantum state engineering methods [7,8,11].

Table 2. Results of the Optimization for Optical Cat States for the Scheme of Fig. 1.^a

state	ε	r_1	θ_1	r_2	θ_2	T	P
$ 0.5\rangle_C$	$1.42 \cdot 10^{-5}$	0.70	5.74	0.32	5.51	0.59	0.153
$ 0.5\rangle_C$	$1.42 \cdot 10^{-5}$	0.58	0	0.66	0	0.40	0.205
$ 0.5\rangle_C$	$1.42 \cdot 10^{-5}$	0.47	0.03	0.28	0.06	0.5	0.110
$ 0.5\rangle_C$	$1.42 \cdot 10^{-5}$	0.68	0	0.46	0	0.5	0.192
$ 0.5\rangle_C$	$1.42 \cdot 10^{-5}$	1.33	0	0	0	0.90	0.033
$ 0.8\rangle_C$	$5.58 \cdot 10^{-4}$	0.40	5.59	0.40	4.53	0.40	0.093
$ 0.8\rangle_C$	$5.58 \cdot 10^{-4}$	0.98	0	0.36	0	0.5	0.199
$ 0.8\rangle_C$	$5.58 \cdot 10^{-4}$	0.86	0	0	0	0.71	0.077
$ 1.0\rangle_C$	$2.89 \cdot 10^{-3}$	0.43	5.54	0.67	4.16	0.36	0.117
$ 1.0\rangle_C$	$2.89 \cdot 10^{-3}$	1.08	0	0.19	0	0.5	0.166
$ 1.0\rangle_C$	$2.89 \cdot 10^{-3}$	1.5	0	0	0	0.67	0.090
$ 1.2\rangle_C$	$9.91 \cdot 10^{-3}$	0.19	1.94	1.32	2.95	0.51	0.153
$ 1.2\rangle_C$	$9.92 \cdot 10^{-3}$	1.02	0	1.5	0	0.22	0.170
$ 1.2\rangle_C$	$9.91 \cdot 10^{-3}$	1.09	0	0	0	0.50	0.125
$ 1.5\rangle_C$	$3.61 \cdot 10^{-2}$	0.61	0.70	0.82	2.75	0.57	0.104
$ 1.5\rangle_C$	$3.61 \cdot 10^{-2}$	0.64	0	0.14	0	0.05	0.029
$ 1.5\rangle_C$	$6.11 \cdot 10^{-2}$	1.5	0	0.01	0	0.5	0.124
$ 1.5\rangle_C$	$3.61 \cdot 10^{-2}$	0.90	0	0	0	0.25	0.113

^aThe table presents for each state the minimal misfit ε and the corresponding optimal choice of parameters: the parameters of the input squeezed vacuum states (r_1 , θ_1 , r_2 , and θ_2), the transmittance of the beam splitter T , and the success probability P . Parameters denoted by bold characters are fixed.

In Table 2, we present the results of the optimization for several examples for the optical cat states prepared in the scheme. As is intuitively expected, the results of the optimization simply reflect that the coherent signal is always zero, that is, the inputs of the scheme are squeezed vacuum states; therefore we omit the parameters of the coherent signals from the table. We also exploit the special characteristics of

the proposed scheme that some of the input parameters can be chosen freely in certain ranges without the significant deterioration of the fidelity, as was pointed out in [16]. Accordingly, we consider cases where the squeezing phases is $\theta_i = 0$ or/and the transmittivity is fixed at $T = 0.5$, and when one of the inputs is the vacuum state, that is, $r = 0$ which was previously excluded from the optimizations. In the latter case, the considered scheme corresponds to the scheme proposed in [33]. The results show that optical cat states can also be generated with high fidelity using the considered scheme. Note that the fidelity decreases with increase in the coherent amplitude. For $\alpha < 1.2$, the probability of success is higher for two squeezed vacuum inputs than that for the case where one of them is a vacuum state. The considered variations of fixing the transmittivity and the phases of squeezing do not change the accuracy of the generation in the considered range of parameters. Finally, we note that owing to the fact that the fidelity and the success probability is high for the low-amplitude cat states in this scheme, optical cat states with larger amplitudes can be successfully prepared with the scheme proposed in [34].

4. Conclusions

We developed a description for the recently introduced single-step traveling-wave quantum state engineering scheme using the one-dimensional coherent state representation introduced by Janszky. Due to its relative simplicity, this description can be advantageously used for numerical optimization aiming at determining the adjustable parameters of the scheme to produce a given target state. We determined the sets of controllable parameters for several examples of amplitude squeezed states, special photon number superpositions, and optical cat states. These state can be produced with high fidelity and success probability.

Acknowledgments

This research was supported by the National Research, Development, and Innovation Office, Hungary (Projects Nos. K124351 and 2017-1.2.1-NKP-2017-00001 HunQuTech). This project was also supported by the European Union, co-financed by the European Social Fund (Grants No. EFOP-3.6.1-16-2016-00004 entitled by Comprehensive Development for Implementing Smart Specialization Strategies at the University of Pécs and No. EFOP-3.6.2-16-2017-00005). P.A. is grateful to József Janszky for his friendship and for the fruitful common work of the past decades.

References

1. J. S. Neergaard-Nielsen, B. M. Nielsen, C. Hettich, et al., *Phys. Rev. Lett.*, **97**, 083604 (2006).
2. A. Ourjoumtsev, H. Jeong, R. Tualle-Brouri, and P. Grangier, *Nature*, **448**, 784 (2007).
3. H. Takahashi, K. Wakui, S. Suzuki, et al., *Phys. Rev. Lett.*, **101**, 233605 (2008).
4. T. Gerrits, S. Glancy, T. S. Clement, et al., *Phys. Rev. A*, **82**, 031802 (2010).
5. J. Etesse, M. Bouillard, B. Kanseri, and R. Tualle-Brouri, *Phys. Rev. Lett.*, **114**, 193602 (2015).
6. K. Huang, H. Le Jeannic, J. Ruaudel, et al., *Phys. Rev. Lett.*, **115**, 023602 (2015).
7. M. Dakna, J. Clausen, L. Knöll, and D.-G. Welsch, *Phys. Rev. A*, **59**, 1658 (1999).
8. J. Fiurášek, R. García-Patrón, and N. J. Cerf, *Phys. Rev. A*, **72**, 033822 (2005).
9. S.-Y. Lee and H. Nha, *Phys. Rev. A*, **82**, 053812 (2010).
10. J. Sperling, W. Vogel, and G. S. Agarwal, *Phys. Rev. A*, **89**, 043829 (2014).

11. E. Molnar, P. Adam, G. Mogyorosi, and M. Mechler, *Phys. Rev. A*, **97**, 023818 (2018).
12. J. Janszky, P. Domokos, and P. Adam, *Phys. Rev. A*, **48**, 2213 (1993).
13. J. Janszky, P. Domokos, S. Szabö, and P. Adam, *Phys. Rev. A*, **51**, 4191 (1995).
14. S. Szabö, P. Adam, J. Janszky, and P. Domokos, *Phys. Rev. A*, **53**, 2698 (1996).
15. P. Adam, E. Molnar, G. Mogyorosi, et al., *Phys. Scr.*, **90**, 074021 (2015).
16. G. Mogyorosi, P. Adam, E. Molnar, and M. Mechler, "Single-step quantum state engineering in traveling optical fields," arXiv:1804.07920 [quant-ph] (2018).
17. J. Janszky and A. V. Vinogradov, *Phys. Rev. Lett.*, **64**, 2771 (1990).
18. P. Adam, J. Janszky, and A. V. Vinogradov, *Opt. Commun.*, **80**, 155 (1990).
19. P. Adam, J. Janszky, and A. V. Vinogradov, *Phys. Lett. A*, **160**, 506 (1991).
20. P. Adam, I. Földesi, and J. Janszky, *Phys. Rev. A*, **49**, 1281 (1994).
21. P. Domokos, P. Adam, and J. Janszky, *Phys. Rev. A*, **50**, 4293 (1994).
22. I. Földesi, P. Adam, and J. Janszky, *Phys. Lett. A*, **204**, 16 (1995).
23. S. Szabö, P. Domokos, P. Adam, and J. Janszky, *Phys. Lett. A*, **241**, 203 (1998).
24. J. Janszky, P. Adam, M. Bertolotti, and C. Sibia, *Quantum Opt.*, **4**, 163 (1992).
25. I. Urizar-Lanz and G. Tóth, *Phys. Rev. A*, **81**, 052108 (2010).
26. P. Adam, M. Mechler, V. Szalay, and M. Koniorczyk, *Phys. Rev. A*, **89**, 062108 (2014).
27. P. Marek and J. Fiurášek, *Phys. Rev. A*, **79**, 062321 (2009).
28. P. Marek, R. Filip, and A. Furusawa, *Phys. Rev. A*, **84**, 053802 (2011).
29. K. Miyata, H. Ogawa, P. Marek, et al., *Phys. Rev. A*, **93**, 022301 (2016).
30. T. C. Ralph, A. Gilchrist, G. J. Milburn, et al., *Phys. Rev. A*, **68**, 042319 (2003).
31. A. P. Lund, T. C. Ralph, and H. L. Haselgrove, *Phys. Rev. Lett.*, **100**, 030503 (2008).
32. D. E. Goldberg, *Genetic Algorithms in Search, Optimization, and Machine Learning*, Addison-Wesley, Boston, MA (1989).
33. M. Dakna, T. Anhut, T. Opatrný, et al., *Phys. Rev. A*, **55**, 3184 (1997).
34. A. P. Lund, H. Jeong, T. C. Ralph, and M. S. Kim, *Phys. Rev. A*, **70**, 020101 (2004).